

Optimization of a Stationary Tomographic MBI System Including Non-Local Means Filtering

Kjell Erlandsson, Andras Wirth, Kris Thielemans, *Senior Member, IEEE*, Ian Baistow, Alexander Cherlin, *Member, IEEE*, Brian F Hutton, *Senior Member, IEEE*

Abstract— A novel stationary tomographic Molecular Breast Imaging (MBI) system is currently under development, with the aim of obtaining high image-quality with low dose and short scanning time. The system is based on dual opposing CZT detector arrays and multi-pinhole collimators. We have recently modified the iterative image reconstruction procedure by incorporating a novel relaxation scheme, in order to make the image contrast and noise properties more uniform throughout the field-of-view. In addition, we have introduced a post-reconstruction image denoising step based on the non-local means (NLM) filter. In view of the significant effect that these steps had on the image quality, we performed a new system parameter optimization. The parameters investigated were pinhole size, opening angle and separation, as well as the number of reconstruction iterations and the degree-of-smoothing parameter of the NLM filter. The optimization was performed based on simulated data, by maximizing the contrast-to-noise ratio (CNR) in the images. We found that the optimal system parameters were not so different with the new data processing steps as compared to previous results, while the CNR was improved by a factor > 3 .

I. INTRODUCTION

MOLECULAR Breast Imaging (MBI) with planar detectors has been proven to have high lesion detection sensitivity in patients with dense breasts, where x-ray mammography has relatively poor performance [1]. However, long scanning times and a relatively high radiation dose are the main obstacles for general acceptance. We have been developing a stationary low-dose MBI system with two opposing cadmium zinc telluride (CZT) detectors with high spatial resolution and depth-of-interaction (DOI) capability [2]. The system is equipped with multi-pinhole (MPH) collimators, allowing for projection-overlap (multiplexing). The image reconstruction procedure incorporates de-multiplexing, aided by the DOI information. The parameters of the system were optimized previously [2]. However, we have now implemented some new data processing steps that affect the image quality and may therefore influence the parameter optimization.

As the spatial resolution and sensitivity depend on the distance from the cameras, the image quality varies over the field-of-view (FOV). In order to address this problem, we have incorporated a relaxation scheme into the reconstruction procedure, which slows down the convergence at the edges of the FOV compared to center.

With low injected activity levels and short acquisition times, a certain level of noise in the reconstructed images is unavoidable, which could affect lesion detection. We therefore applied a non-local means (NLM) filter [3] to the reconstructed images, resulting in significant noise-reduction.

The objective of this paper is to present simulation studies performed to optimize the system design parameters when the above-described data processing steps were included.

II. METHODS

The system consists of two 16 x 16 cm detectors with 7.3 mm thick CZT crystals (Fig. 1). The pixel size and DOI resolution were 1 mm. The collimators were made of 5 mm thick Tungsten with arrays of square-shaped pinholes. The system geometry was designed such that projections from different pinholes would overlap on the detectors (multiplexing, MX). This leads to higher photon detection efficiency and improved sampling, but also to uncertainty regarding the path of each detected photon and possible artefacts. The MX effect was incorporated into the system matrix used for forward- and back-projection during reconstruction.

Simulations were performed for a 6-cm thick phantom consisting of a uniform background with two sets of 7 spherical inserts in different planes, one set close to the edge ($y=-24.5$ mm) and one close to the center of the FOV ($y=5.5$ mm) (Fig. 2). The insert diameters were in the range 4-10 mm and the target-to-background ratio was 10. Poisson noise was added to the projection data, assuming an injected activity of 150 MBq and an acquisition time of 2.5 min.

The relaxation scheme for the image reconstruction process is described by the following equation:

$$f^{k+1}(\mathbf{r}) = f^k(\mathbf{r}) \cdot (q_{EM}^k)^{\tau(y)}, k > 1$$

which represents the standard ML-EM update step, where q_{EM}^k is the update factor at iteration k and $\tau(y)$ is the relaxation factor, dependent on the coordinate y (see Fig. 1). τ decreases linearly from 1 at the center to 0.1 at the edge of the FOV (Fig. 3). The image reconstruction was performed with 15 iterations and 3 subsets, defined on the DOI-level. The matrix size was 160x160x60 and the voxel size 1 mm cubed.

For the NLM-filter, we used a MATLAB function (Mathworks, Natick MA, USA), which operates in 2D. The

filter was applied to each x - z image plane independently with a search window size of 127, a comparison-window size of 13 and a variable degree-of-smoothing (DOS) (see below).

The parameters investigated (and corresponding ranges) were pinhole size (1.5-2.0 mm), opening angle (80-95°) and separation (7-13 mm), number of iterations (1-15) and the filter DOS (5-100).

The contrast-to-noise ratio (CNR) was calculated for each sphere. The objective function to be maximized was defined as:

$$O = \frac{\overline{C_{5,6}^E}}{2} + \overline{C_{6,7}^C}$$

where C_d^y is the CNR value for the sphere of diameter d (mm) at position y (Edge/Centre). This was done in order to optimize for the detection of small lesions, while taking into account the difference in resolution between the edge and the center of the FOV.

III. RESULTS

The effect of the relaxation scheme can be seen in Fig. 4, showing CNR in each sphere in the two planes as a function of iterations with and without relaxation. The convergence rate slows down in the edge plane, becoming similar to that in the centre plane.

Figure 5 shows reconstructed images for two planes of the simulated phantom, without and with NLM-filtering. The NLM filter results in a significant reduction of background noise without, in most cases, affecting the contrast. This makes the lesions more conspicuous.

The outcome of the optimization is presented in Table I. The optimal values for the different parameters with and without NLM-filter are not so different from each other, nor from previous results. A slightly larger pinhole size was obtained with filter, corresponding to higher sensitivity. This would be compensated for by a larger pinhole separation, which also results in less multiplexing. The objective function value was over twice as high with the NLM-filter and the average CNR in all lesions was improved by a factor of 3.7.

IV. DISCUSSION & CONCLUSIONS

Our results show that 1) the relaxation scheme can even out the convergence rate between regions of the FOV with different sensitivity and resolution, 2) the NLM filter can significantly reduce the background noise without affecting the lesion contrast in most cases, and 3) system parameter optimization was not overly affected by these two processing steps. The NLM post-filtering resulted in an increased CNR by over a factor of 3.

REFERENCES

- [1] C. B. Hruska, "Molecular Breast Imaging for Screening in Dense Breasts: State of the Art and Future Directions", *AJR*, 2017; 208:275-83, 2017.
- [2] K. Erlandsson, A. Wirth, K. Thielemans, I. Baistow, A. Cherlin, B. F. Hutton, "Design of a low-dose, stationary, tomographic Molecular Breast Imaging system using 3D position sensitive CZT detectors", *IEEE TRPMS* in press, 2022.
- [3] A. Buades, B. Coll, J.-M. Morel, "A non-local algorithm for image denoising", *IEEE Comp. Soc. Conf. CVPR*, 2:60-5, 2005.

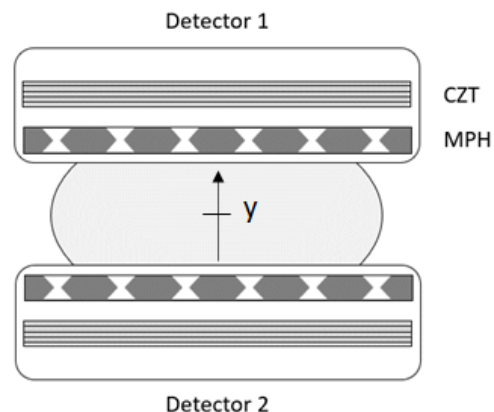


Fig. 1. Conceptual design of the stationary MBI detector system with two CZT detectors and multi-pinhole collimators. The y -coordinate is perpendicular to the detector surfaces, as indicated.

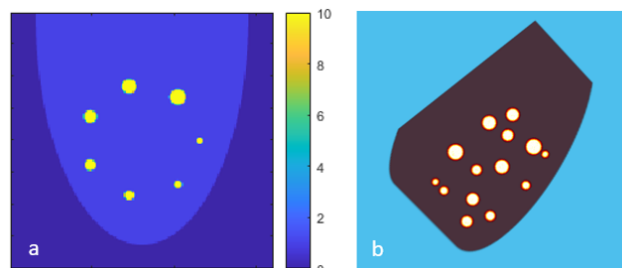


Fig. 2. Phantom with two layers of 7 spherical inserts; a) transaxial (x - z) plane, b) maximum-intensity projection at an oblique angle, showing all spheres.

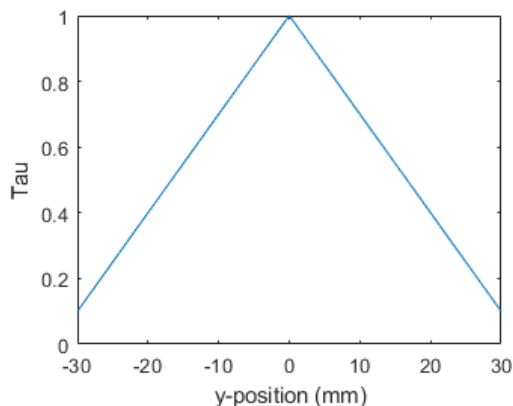


Fig. 3. Relaxation factor as a function of the y -coordinate.

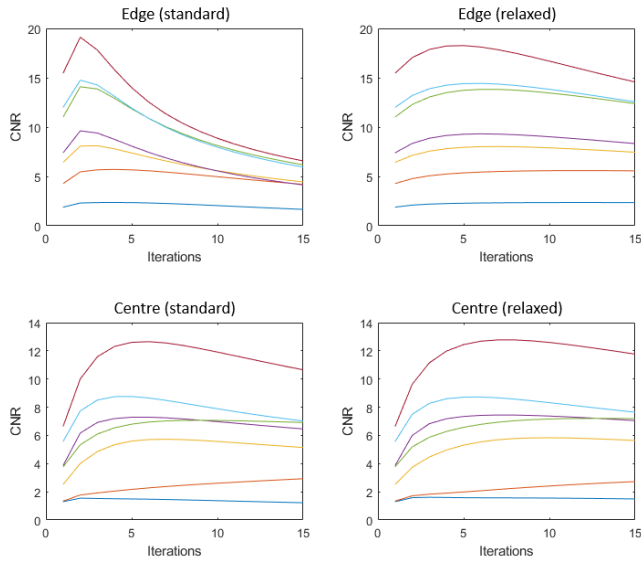


Fig. 4. CNR as a function of iterations for spheres in the edge (top row) and centre plane (bottom row) without (left column) and with relaxation scheme (right column).

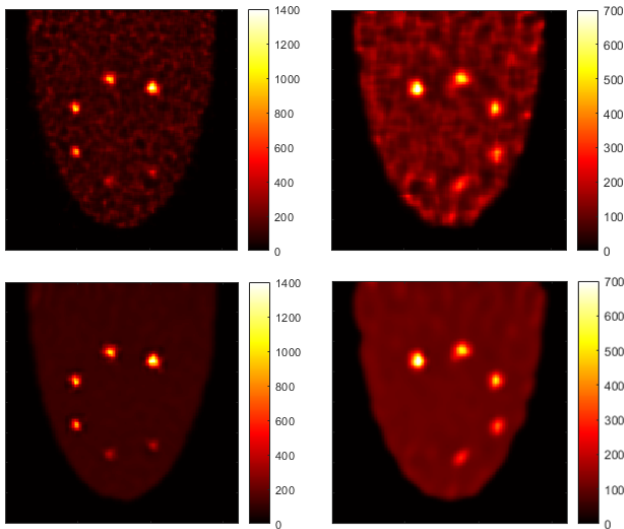


Fig. 5. Reconstructed images of the simulated phantom for two planes, $y=6$ (left column) and $y=36$ (right column), without (top row) and with NLM-filtering (bottom row).

Table I. Optimized parameters from previous work and the current work, without and with NLM-filter, including objective function values and average CNR.

	Previous	No filter	NLM-filter
PH angle (°)	85	90	90
PH size (mm)	1.75	1.5	1.75
PH sep. (mm)	9	9	10
N-iter.		15	15
DOS		-	35
O		4.01	8.47
CNR		8.01	29.5